Available online at www.sciencedirect.com

ScienceDirect

Energy Procedia 142 (2017) 374–380

Energy Procedia

www.elsevier.com/locate/procedia

9th International Conference on Applied Energy, ICAE2017, 21-24 August 2017, Cardiff, UK

Simulation study of Ferricyanide/Ferrocyanide concentric annulus thermocell with different electrode spacing and cell direction

Gao Qian [a], Yiji Lu [b], Yuqi Huang [a,*], Zhi Li [a], Xiaoli Yu [a], Anthony Paul Roskilly [b]

[a] College of Energy Engineering, Zhejiang University, Hangzhou 310027, China
[b] Sir Joseph Swan Centre for Energy Research, Newcastle University, Newcastle Upon Tyne, NE1 7RU, UK

Abstract

Thermogalvanic cell also named as thermocell is a new type of technology converting low-grade thermal energy to electricity. In this study, we establish an one-dimensional model of a $Fe(CN)_6^{3-/4-}$ concentric annulus thermocell and evaluate the influence of electrode spacing and cell direction on the cell performance. Results indicate the ratio of electrolyte thermal resistance to total thermal resistance plays a crucial role in cell performance while electric resistance has relatively less influence. The power of thermocell rises significantly as the electrode spacing increases, from about 0.75mW in both directions to 1.75 mW in horizontal direction and 2.75 mW in vertical direction. Convection of electrolyte is unfavorable to cell performance and the critical electrode spacing where convection begins to affect heat transfer is predicted to be the optimized spacing. At all values of electrode spacing in this study, thermocell in vertical direction performs better than that of horizontal direction.

Peer-review under responsibility of the scientific committee of the 9th International Conference on Applied Energy.

Keywords: thermocell, thermal resistance analysis, one-dimensional model

* Corresponding author. Tel.: +86 (0) 135 8821 1971
E-mail address: huangyuqi@zju.edu.cn (Y. Huang)

1876-6102
Peer-review under responsibility of the scientific committee of the 9th International Conference on Applied Energy.
10.1016/j.egypro.2017.12.059

1. Introduction

To solve energy crisis and environment deterioration, technologies for utilizing low-grade heat source such as thermoelectric power generation [1, 2], sorption technologies [3-5] and Organic Rankine cycle [6-8], have been widely investigated around the world. In addition to these, a novel technology named as 'thermogalvanic cell' or 'thermocell' has recently receiving increasing attentions for low-grade energy application [9-11]. Thermocell can convert the heat source lower than 100 °C with aqueous electrolyte into electricity driven by the temperature difference between the two half-cells [12]. The thermocell technology has the advantages of no requirement of moving parts, directly converting heat energy into electricity and much higher seebeck coefficiency (>1 mV/K) compared with conventional thermoelectric power generation system [13]. Moreover, thermocell is made of liquid electrolyte so that it can be fabricated into a good many shapes such as flexible thin films [14]. Additionally, when thermocell is used in thermally regenerative electrochemical cycle (TREC), a high heat-to-electricity energy conversion efficiency of 5.7% can be achieved when cycled between 10 and 60 ^{o}C [15].

The majority research efforts are currently focusing on the investigation of single cell performance and development of new materials for thermocell technology [16-18]. However, the geometry and cell directions of thermocell play significant roles on the performance of thermocell. The previous reported studies on the cell prototype use the same and invariable two electrode surface areas and set the temperature of electrodes in constant value [11, 16, 19], which cannot represent the realistic application conditions of this technology. The thermocell in application is usually designed as concentric annulus [20], whose areas of electrode surface are not the same and dependent on the radius of pipe. And only the temperatures of cold and heat source are controlled. Temperatures of electrodes are highly relative to heat transfer through the cell which is determined by the geometry and cell direction. Fig.1 represents the structure of concentric annulus thermocell. In this study, a one-dimensional simulation model has been conducted to investigate the effects of electrode spacing and cell direction for a $Fe(CN)_6^{3-/4-}$ thermocell using concentric annulus geometry in order to study the heat transfer performance and energy conversion efficiency of this technology.

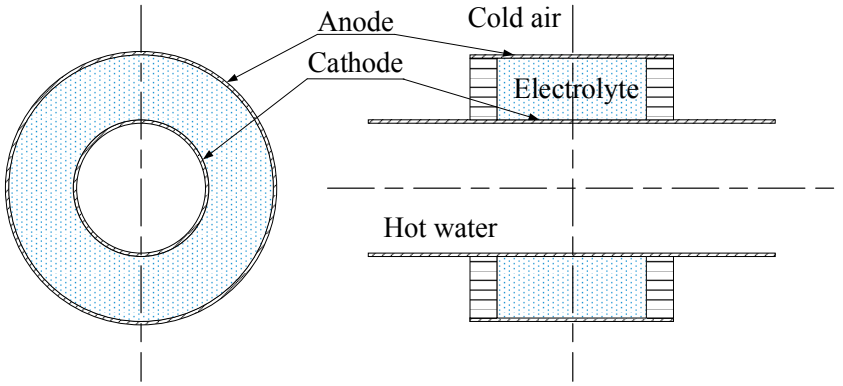

Fig. 1. Structure of concentric annulus thermocell

2. Description of the simulation model

Fig. 2 shows the schematic diagram of the thermocell simulation model using thermal resistance analysis. Several assumptions have been made in this study to simplify the cell model.

- The pipe walls and electrodes are considered thin enough so as to neglect their influence on heat transfer.
- The flow of hot water in the inner pipe is regarded as fully developed laminar flow.
- The electrolyte inside the cell may stay still or have a circulation, which depends on the Rayleigh number of the fluid. Natural convection occurs outside the outer pipe wall.
- In order to simplify the wall temperature as uniform without the temperature difference between the inlet and outlet, the length of cell L should not be too large (10cm in this study).

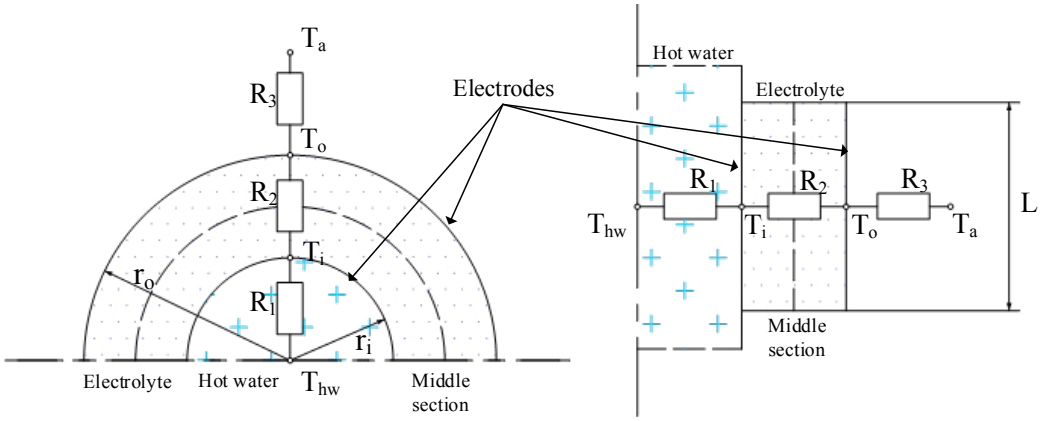

(a) (b)

Fig. 2. Schematic diagram of concentric annulus thermocell model
(a) Horizontal direction, (b) vertical direction

With these assumptions, the one-dimensional heat transfer model can be established with thermal resistance theory. Two cell orientations are considered, in horizontal and vertical direction. r_i is set at 5cm and r_o is a variable parameter. The dash line between the inner and outer walls stands for the middle section of the cell which is used in the calculation as introduced below. Temperature of hot water is set at 313.1K and temperature of air outside the pipe is 293.1K.

3. Methodologies

3.1. Heat to electricity

Mua et al. present the performance features of $Fe(CN)_6^{3-/4-}$ thermocell [21]. The *E-I* curves of $Fe(CN)_6^{3-/4-}$ thermocell is nearly linear so that the max power of the thermocell can be expressed as equation (1). The total cell resistance comprises three parts, ohmic resistance, activation resistance and mass transport resistance. Among these three parts of resistance, ohmic resistance is the largest part and the other two are negligible when the electrode separation is small. Therefore the total cell resistance can be approximately replaced by the ohmic resistance as is shown in equation (2). The sectional area of the cell between two electrodes, A_{sec}, is simplified to the area of a cylindrical middle section surface with radius equals to $(r_o+r_i)/2$. Additionally, Hu et al.'s [13] research shows that the dependence of open voltage on temperature in thermocell is linear which means the Seebeck coefficient of the thermocell is almost constant. Hence the open-circuit voltage can be calculated as equation (3), where ΔT is the temperature difference of two electrodes. The values of σ and S are provided from these papers [13, 21].

$$P_{\max} \approx \frac{1}{4} V_{oc} I_{sc} = \frac{V_{oc}^2}{4R_{cell}} \tag{1}$$

$$R_{cell} \approx \frac{r_o - r_i}{\sigma A_{\sec}} \tag{2}$$

$$V_{oc} \approx S\Delta T \tag{3}$$

To raise the output power of thermocell, high temperature difference of electrodes and low electric resistance need to be achieved.

3.2. Heat transfer equations

Horizontal direction

Forced convection resistance inside the inner pipe is given by equation (4), where h_i is determined by the Nusselt number. Because it is fully developed laminar flow in the circle pipe, Nu=4 is reasonable here [22].

Thermal resistance in the cell is given by equation (5) where the k_{eff} is the effective thermal conductivity of electrolyte given by equation (6), and the characteristic length L_c used for calculating Rayleigh number is given by equation (7) [22]. Particularly when $k_{eff} < k_e$, the value of k_{eff} have to equal to that of k_e, which means there is only heat conduction through the cell. Equation (6) is applicable for $0.7 \leqslant Pr_e \leqslant 6000$ and $Ra_e \leqslant 10^7$. Since the thermal properties of electrolyte are not found in previous papers, the electrolyte is regarded as pure water here.

$$R_1 = \frac{1}{h_i A_i} \tag{4}$$

$$R_2 = \frac{\ln(r_o/r_i)}{2\pi L k_{eff}} \tag{5}$$

$$k_{eff} = 0.386\left(\frac{Pr_e}{0.861+Pr_e}\right)^{1/4} Ra_e^{1/4} k_e \tag{6}$$

$$L_c = \frac{2\left[\ln(r_o/r_i)\right]^{4/3}}{\left(r_i^{-3/5}+r_o^{-3/5}\right)^{5/3}} \tag{7}$$

Natural convection resistance outside the outer pipe is given by equation (8), and the corresponding Nusselt number is given by equation(9) which is applicable for $Ra_a \leqslant 10^{12}$ [22].

$$R_3 = \frac{1}{h_o A_o} \tag{8}$$

$$Nu_a = \left\{0.6 + \frac{0.387 Ra_a^{1/6}}{\left[1+(0.559/Pr_a)^{9/16}\right]^{8/27}}\right\}^2 \tag{9}$$

Vertical direction

Forced convection resistance inside the inner pipe is same as horizontal type. Thermal resistance in the cell is firstly calculated by empirical formula for rectangular cavity, but in this study, the Rayleigh numbers of electrolyte calculated in all conditions are below the critical value 1000 so that there is only heat conduction in the cell. R_2 is given by equation (10). Nusselt number of cool air is given by equation (11) [22], which is applicable for $Ra_a \leqslant 10^9$.

$$R_2 = \frac{\ln(r_o/r_i)}{2\pi L k_e} \tag{10}$$

$$Nu_a = \left\{0.825 + \frac{0.387 Ra_a^{1/6}}{\left[1+(0.492/Pr_a)^{9/16}\right]^{8/27}}\right\}^2 \tag{11}$$

3.3. Efficiency of energy conversion

Total thermal resistance R_{total} is the sum of R_1, R_2, R_3 and the heat transferred through the system is calculated by $Q=(T_{hw}-T_a)/R_{total}$. The temperature difference of two electrodes is given by $\Delta T=T_i-T_o=QR_2$. The efficiency of energy conversion η is the ratio of P_{max} and Q. Since ΔT is not constant here, relative efficiency $\eta_r = \eta/\eta_{carnot}$ is used to evaluate the cell performance.

4. Results and discussion

To solve this model, iterative algorithm is used and the iteration variables are T_i and T_o. Non-dimensional numbers and thermal properties in this model are calculated from appendixes [22] by linear interpolation method and the fluid temperatures are approximated as arithmetic mean temperatures of the hot and cold sides. For example, temperature of electrolyte is considered as $(T_i+T_o)/2$. Electrode spacing is normalised as the ratio of spacing and inner radius.

4.1. Analysis of heat transfer

The dependence of thermal resistance on electrode spacing is shown in Fig. 3(a). With the increase of electrode spacing, $R_{2,H}$ and $R_{2,V}$ are both rising and keep the same at the beginning until the normalised electrode spacing reaches 2, after which $R_{2,H}$ starts to be smaller than $R_{2,V}$. As is mentioned above, there is only heat conduction for $R_{2,V}$ while what type of heat transfer for $R_{2,H}$ depends on the value of k_{eff}. When electrode spacing is larger than 2, $k_{eff} > k_e$, which means that convection begins to influence the heat transfer. $R_{3,H}$ is larger than $R_{3,V}$ and both of them drop continually in a similar trend, resulted from the increase of A_o. Although there are apparent variation in these

thermal resistance, the total $R_{total,H}$ is larger than $R_{total,V}$ at first and after convection affecting heat transfer, $R_{total,H}$ declines obviously. When the spacing is about 2.75, $R_{total,H}$ becomes smaller than $R_{total,V}$.

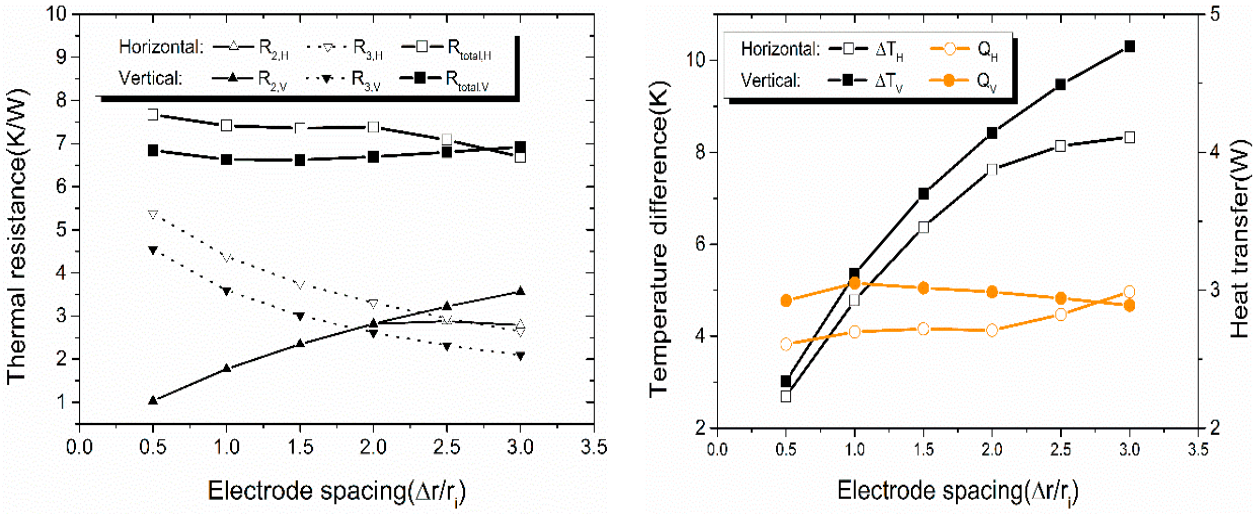

(a) (b)

Fig. 3. (a) Diagram of thermal resistance; (b) Diagram of temperature difference and heat transfer

Thermal resistance determines heat going through the thermocell and temperature difference of electrodes, and the variation trend is show in Fig. 3(b). Larger thermal resistance means fewer heat transferred, hence the trend of Q is opposite to that of R_{total}. Temperature difference of electrodes is related to R_2/R_{total} so that $\Delta T_H < \Delta T_V$ and both of them rise greatly from about 3K to over 8K. The difference between ΔT_H and ΔT_V becomes larger as electrode spacing increases and convection of electrolyte in horizontal direction makes the difference much bigger.

4.2. Analysis of efficiency

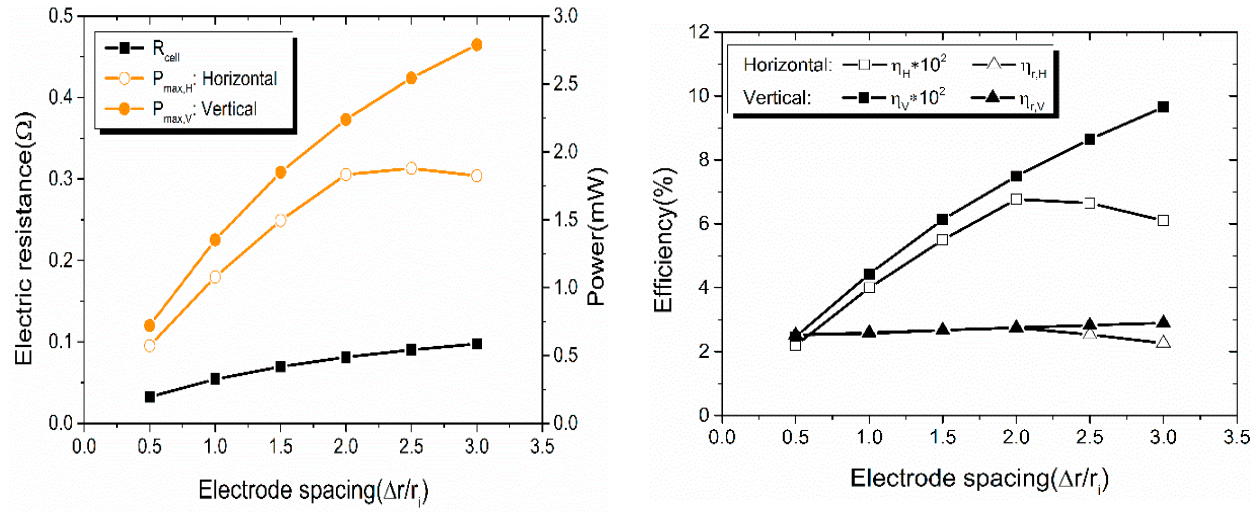

(a) (b)

Fig. 4. (a) Diagram of electric resistance and power; (b) Diagram of efficiency and relative efficiency

Fig. 4(a) illustrates the variation of electric resistance and the max output power of thermocell. Due to the simplification of the thermocell, electric resistance is the same in this study and it is growing steadily. The trend of P_{max} is similar to that of ΔT meaning that grow of electric resistance is not as dominant to the performance of thermocell as the variation of thermal resistance. Note that the increase of power in horizontal direction slows down significantly after convection occurs, and the power starts to drop when electrode spacing reaches 2.5.

The similar trend occurs on the efficiency of energy conversion as Fig. 4(b). To explain this, we should look back to the thermal resistance curves. In spite of apparent variation of R_2 and R_3, the total thermal resistance merely changes to a small extent, leading to the steady Q curves. Therefore, the change of efficiency depend mainly on output power. By contrast, the relative efficiencies of both directions are almost the same before convection affects heat transfer in horizontal direction.

5. Conclusions

We have investigated the influence of electrode spacing and cell directions on the performance of thermocell with a simplified one-dimensional analytical model. Six values of electrode spacing and two directions (horizontal and vertical) are discussed and evaluated in this study. After solving the model by iterative algorithm, discussion has been made on heat transfer, electric properties of thermocell and the efficiency of energy conversion. Several conclusions are drawn as follows:

1. Organising the distribution of thermal resistances is an effective way to optimise the cell because thermal resistance plays an important role in the performance of thermocell. Total thermal resistance determines the heat through the cell and the distribution of thermal resistances determines the difference of temperature between two electrodes. In order to have higher power, more investigations ought to be carried out to raise the value of R_2/R_{total}. Although electric resistance is also changes the influence on the cell is not as crucial as thermal resistance.
2. Increasing electrode spacing is one of effective approaches to optimise the distribution of thermal resistances and by this way the power of thermocell increases from about 0.75 mW in both directions to 1.75 mW in horizontal direction and 2.75mW in vertical direction in this study. Convection of electrolyte is unfavourable here for that it decreases the thermal resistance of electrolyte. The critical point between convection and pure conduction is predicted to be the optimal point where thermocell will have the best performance.
3. In the range of this study, vertical direction shows better performance than horizontal direction at every value of electrode spacing. And the critical point of vertical direction does not appear.

More investigation work will be carried out to verify the results and improve the accuracy of the simulation model. The length of the thermocell is also an important parameter because it influences the electrolyte convection and the temperature distribution is not negligible when the length is big enough.

Acknowledgements

The authors also would like to thank the support from NSFC-RS Joint Project under the grant number No. 5151101443 and IE/151256.

References

[1] R. Stobart, M.A. Wijewardane, Z. Yang, Comprehensive analysis of thermoelectric generation systems for automotive applications, Applied Thermal Engineering, 112 (2017) 1433-1444.
[2] H. Ali, B.S. Yilbas, A. Al-Sharafi, Innovative design of a thermoelectric generator with extended and segmented pin configurations, Applied Energy, 187 (2017) 367-379.
[3] S.M. Ali, A. Chakraborty, Thermodynamic modelling and performance study of an engine waste heat driven adsorption cooling for automotive air-conditioning, Applied Thermal Engineering, 90 (2015) 54-63.

[4] Y. Lu, Y. Wang, H. Bao, L. Wang, Y. Yuan, A.P. Roskilly, Analysis of an optimal resorption cogeneration using mass and heat recovery processes, Applied Energy, 160 (2015) 892-901.
[5] Y. Lu, A.P. Roskilly, K. Tang, Y. Wang, L. Jiang, Y. Yuan, L. Wang, Investigation and performance study of a dual-source chemisorption power generation cycle using scroll expander, Applied Energy, epub ahead of print (2017).
[6] A. Uusitalo, J. Honkatukia, T. Turunen-Saaresti, Evaluation of a small-scale waste heat recovery organic Rankine cycle, Applied Energy, 192 (2017) 146-158.
[7] Y. Lu, A.P. Roskilly, A. Smallbone, X. Yu, Y. Wang, Design and parametric study of an Organic Rankine cycle using a scroll expander for engine waste heat recovery, Energy Procedia, 105C (2017) 1421-1426.
[8] Y. Lu, A.P. Roskilly, X. Yu, K. Tang, L. Jiang, A. Smallbone, L. Chen, Y. Wang, Parametric study for small scale engine coolant and exhaust heat recovery system using different Organic Rankine cycle layouts, Applied Thermal Engineering, 127 (2017) 1252-1266.
[9] T.J. Abraham, D.R. MacFarlane, R.H. Baughman, L. Jin, N. Li, J.M. Pringle, Towards ionic liquid-based thermoelectrochemical cells for the harvesting of thermal energy, Electrochimica Acta, 113 (2013) 87-93.
[10] A. Gunawan, C.-H. Lin, D.A. Buttry, V. Mujica, R.A. Taylor, R.S. Prasher, P.E. Phelan, Liquid Thermoelectrics: Review of Recent And Limited New Data of Thermogalvanic Cell Experiments, Nanoscale and Microscale Thermophysical Engineering, 17 (2013) 304-323.
[11] P.F. Salazar, S. Kumar, B.A. Cola, Design and optimization of thermo-electrochemical cells, Journal of Applied Electrochemistry, 44 (2014) 325-336.
[12] T.J. Kang, S. Fang, M.E. Kozlov, C.S. Haines, N. Li, Y.H. Kim, Y. Chen, R.H. Baughman, Electrical Power From Nanotube and Graphene Electrochemical Thermal Energy Harvesters, Advanced Functional Materials, 22 (2012) 477-489.
[13] R. Hu, B.A. Cola, N. Haram, J.N. Barisci, S. Lee, S. Stoughton, G. Wallace, C. Too, M. Thomas, A. Gestos, Harvesting waste thermal energy using a carbon-nanotube-based thermo-electrochemical cell, Nano Letters, 10 (2010) 838.
[14] H. Im, H. Moon, J. Lee, I. Chung, T. Kang, Y. Kim, Flexible thermocells for utilization of body heat, Nano Research, 7 (2014) 443-452.
[15] S.W. Lee, Y. Yang, H.-W. Lee, H. Ghasemi, D. Kraemer, G. Chen, Y. Cui, An electrochemical system for efficiently harvesting low-grade heat energy, (2014).
[16] A. Gunawan, H. Li, C.H. Lin, D.A. Buttry, V. Mujica, R.A. Taylor, R.S. Prasher, P.E. Phelan, The amplifying effect of natural convection on power generation of thermogalvanic cells, International Journal of Heat & Mass Transfer, 78 (2014) 423-434.
[17] M.S. Romano, N. Li, D. Antiohos, J.M. Razal, A. Nattestad, S. Beirne, S. Fang, Y. Chen, R. Jalili, G.G. Wallace, R. Baughman, J. Chen, Carbon Nanotube – Reduced Graphene Oxide Composites for Thermal Energy Harvesting Applications, Advanced Materials, 25 (2013) 6602-6606.
[18] V. Zinovyeva, S. Nakamae, M. Bonetti, M. Roger, Enhanced Thermoelectric Power in Ionic Liquids, CHEMELECTROCHEM, 1 (2014) 426-430.
[19] T.I. Quickenden, Y. Mua, The Power Conversion Efficiencies of a Thermogalvanic Cell Operated in Three Different Orientations, Journal of the Electrochemical Society, 142 (1995) 3652-3659.
[20] A. Gunawan, N.W. Fette, P.E. Phelan, Thermogalvanic Waste Heat Recovery System in Automobiles, in: ASME 2015 Power Conference Collocated with the ASME 2015 International Conference on Energy Sustainability, the ASME 2015 International Conference on Fuel Cell Science, Engineering and Technology, and the ASME 2015 Nuclear Forum, 2015, pp. V001T011A002.
[21] Y. Mua, T.I. Quickenden, Power Conversion Efficiency, Electrode Separation, and Overpotential in the Ferricyanide/Ferrocyanide Thermogalvanic Cell, Journal of the Electrochemical Society, 143 (1996) 2558-2563.
[22] F.P. Incropera, D.P. DeWitt, T.L. Bergman, A.S. Lavine, Fundamentals of Heat and Mass Transfer, 6th ed., John Wiley & Sons, 2006.